# Revisiting PbTe to identify how thermal conductivity is really limited

Shenghong Ju,[1,2] Takuma Shiga,[1] Lei Feng,[1] and Junichiro Shiomi[1,2,3,*]

[1]*Department of Mechanical Engineering, The University of Tokyo, 7-3-1 Hongo, Bunkyo, Tokyo 113-8656, Japan*

[2]*Center for Materials research by Information Integration, National Institute for Materials Science (NIMS), 1-2-1 Sengen, Tsukuba, Ibaraki 305-0047, Japan*

[3]*Core Research for Evolutional Science and Technology (CREST), Japan Science and Technology Agency (JST), 4-1-8, Kawaguchi, Saitama 332-0012, Japan*

(Received 4 December 2017; revised manuscript received 27 March 2018; published 14 May 2018)

Due to the long range interaction in lead telluride (PbTe), the transverse optical (TO) phonon becomes soft around the Brillouin zone center. Previous studies have postulated that this zone-center softening causes the low thermal conductivity of PbTe through either enlarged phonon scattering phase space and/or strengthened lattice anharmonicity. In this paper, we reported an extensive sensitivity analysis of the PbTe thermal conductivity to various factors: range and magnitude of harmonic and anharmonic interatomic force constants and phonon wave vectors in the three-phonon scattering processes. The analysis reveals that the softening by long range harmonic interaction itself does not reduce thermal conductivity, and it is the large magnitude of the anharmonic (cubic) force constants that realizes low thermal conductivity, however, not through the TO phonons around the zone center but dominantly through the ones with larger wave vectors in the middle of Brillion zone. The paper clarifies that local band softening cannot be a direct finger print for low thermal conductivity and that the entire Brillion zone needs to be characterized on exploring low thermal conductivity materials.

DOI: 10.1103/PhysRevB.97.184305

## I. INTRODUCTION

Thermal transport in crystals with strong lattice anharmonicity has attracted great attention as a source of anomalous high-order lattice dynamics and means to realize thermoelectrics with low intrinsic thermal conductivity. Lead telluride (PbTe) is the most studied material, owning to its high thermoelectric performance [1] and high structural-symmetry enabling in-depth analysis and detailed experimental characterization [2]. The measured bulk thermal conductivity of single crystal PbTe is around 2.2 $Wm^{-1}K^{-1}$ [3–5] at room temperature. This is extremely low compared with other high-symmetry thermoelectric crystals that, to achieve similar thermal conductivity, need to be nanostructured in forms of alloys [6,7], superlattices [8,9], and nanocrystals [10,11].

Over the last decade, there has been a great advance in associating this low thermal conductivity to anharmonic lattice dynamics characteristics. The transverse optical (TO) phonon at Γ point is extremely soft and has a relatively low frequency [12–16] and exhibits a diverging Grüneisen parameter [14,17]. The high sensitivity of the Γ-TO mode to the volume change suggested large coupling between the TO modes and longitudinal acoustic (LA) modes [12], and the intrinsic scattering of LA modes would pull down the thermal conductivity. This was later quantified by first-principles anharmonic lattice dynamics [17], which showed that TO phonons overall are responsible for 61.5% of the scattering rates of LA phonons whose contribution to thermal conductivity is consequently limited to 21%. Detailed inelastic neutron scattering also supports the anharmonic TO-LA interaction through broadened line shapes and avoided crossing [2].

An important point here is that anharmonic features, including non-Gaussian radial distribution function (RDF) in neutron diffraction [18] and double peaks in neutron scattering [2,19,20], can be reproduced by first-principles anharmonic lattice dynamics method, and thus they can be captured by perturbation theory [21]. The perturbation analysis has revealed an important role of certain interatomic force constants (IFCs). Non-Gaussian RDF and the double-peak line shape mainly originate from the nearest-neighbor cubic IFCs in the [100] direction, whose magnitude is considerably larger than other cubic IFCs. The softening of TO modes was attributed to long range harmonic IFCs in the [100] direction with large magnitude because of the resonant bonding: it was introduced by long-range polarization of *p*-electron distribution to atomic displacement, which was found to be a common feature in lead chalcogenides [22].

Besides the above, it has been shown that as temperature increases and the TO mode stiffens, the phase space for scattering between the TO and acoustic phonons disappears, which weakens the temperature dependence of thermal conductivity [23]. Anomalous splitting of the spectrum at the zone center captured by both inelastic neutron scattering measurements [2] and first-principles calculations [20] was found to be related with the nearest neighbor cubic and quartic anharmonic interaction. There has also been an experimental report showing that the lead ion in PbTe and PbS is on average displaced by 0.2 Å from the rock-salt lattice position, which can cause phonon scattering [24].

As above, a good progress has been made to characterize and understand the origin of specific features of harmonic

*Corresponding author: shiomi@photon.t.u-tokyo.ac.jp

 

and anharmonic lattice dynamics; however, the way in which that actually contributes to low thermal conductivity remains vague. Soft zone-center TO mode with large Grüneisen number has been suggested to play the core role, but it is not clear at this point whether the role is to increase the scattering phase space (SPS) or to increase the scattering magnitude. Moreover, there is a question as to whether the softening of the modes around the zone center would have a significant impact on a broad range of modes in the Brillion zone that contribute to thermal conductivity. Clarifying these points is important as it influences the strategy in looking for low thermal conductivity materials. In this paper, we conduct a sensitivity study of PbTe thermal conductivity with respect to participation of specific range of IFCs and phonon modes in the entire first Brillion zone to identify their contribution to thermal conductivity.

## II. METHODOLOGY

The calculations are based on lattice dynamics using IFCs obtained from first principles. We adopted $4 \times 4 \times 4$ conventional supercell containing 512 atoms, which is larger than any system used in previous calculations [17,21,22,25], to ensure that the calculated system fully captures the long range interaction. Both harmonic and anharmonic IFCs were calculated by density functional theory (DFT) and the real-space displacement method [26,27] using Quantum ESPRESSO [28] and ALAMODE [29] packages. Including spin-orbit coupling (SOC) leads to softening of all phonon modes and improves the agreement with experimental dispersion relations [30]. The effect of SOC on thermal conductivity calculation has been discussed in a previous work [25]. By considering the SOC effect, the relaxation time of all phonon modes are noticeably larger, which results in larger thermal conductivity than that without SOC effect at room temperature. In this paper, we used the Perdew-Zunger norm conserving pseudopotentials incorporating relativistic effects [31], which includes the SOC effect under the local density approximation (LDA) for electron exchange-correlation potential. The energy cutoff of 60 Ryd were used for DFT calculations, and the lattice constant after total energy minimization is 6.289 Å. The $k$ mesh used in the calculation is $2 \times 2 \times 2$ for the conventional supercell. The effect of ionic charges in PbTe was considered by performing density functional perturbation theory (DFPT) calculation [30–32]. The obtained phonon dispersion of PbTe along high symmetry lines is shown in Fig. 1(a). Although TO frequency at zone center is larger than that of the experiment [15] by about 0.4 THz, which could be attributable to the use of ground-state harmonic force constants, the overall feature agrees reasonably well with the experimental results [15] as well as previous first-principle calculations [22]. We also performed the calculations for different sizes of supercell using the supercell approach (see Figs. S1 and S2 in the Supplemental Material [33]); it is shown that the dispersion relations and the TO frequency at the zone center approach the DFPT results with the increasing size of the supercell. One drawback of the supercell approach is that large supercells are needed to calculate the IFCs accurately. In this paper, we adopted $4 \times 4 \times 4$ supercell, which is the maximum size that accessible computers could afford, to capture the long range lattice dynamics in PbTe. Particularly, we compared the TO

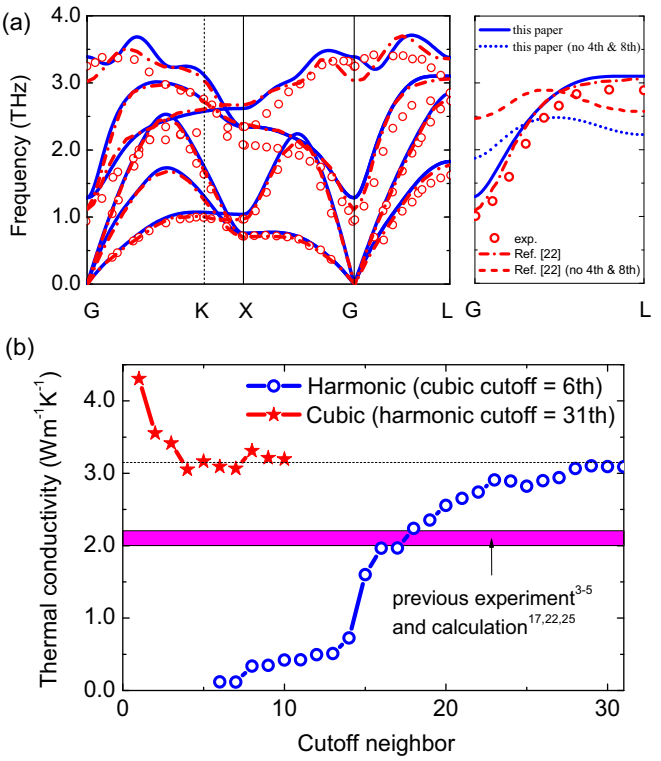


FIG. 1. (a) Phonon dispersion of PbTe from first-principles calculation in this paper (solid line), Lee *et al.* [22] (dashed-dotted line), and experiments [15] (open circles). The TO phonon dispersion along [100] direction with and without the long range of fourth and eighth neighbor harmonic force constants is also shown, where solid and dot lines are from current calculations and dash-dot and dash lines are from Ref. [22]. (b) Thermal conductivity of PbTe at room temperature versus the cutoff distance of harmonic and cubic forces.

phonon dispersion along [100] direction with that of Lee *et al.* [22] by turning off the fourth and eighth neighbor harmonic force constants, which results in a similar nondispersive TO branch. The minor difference in amplitude possibly comes from the difference in the pseudopotentials used.

The Boltzmann transport equation (BTE) with relaxation time approximation (RTA) [26,34,35] was employed to calculate the lattice thermal conductivity,

$$\kappa_{\alpha\beta} = \frac{1}{\Omega N_q} \sum_{\boldsymbol{q},j} c_{\boldsymbol{q}j} v^{\alpha}_{\boldsymbol{q}j} v^{\beta}_{\boldsymbol{q}j} \tau_{\boldsymbol{q}j}, \tag{1}$$

where $\Omega$ is the volume of the primitive unit cell; $N_q$ is the number of $q$ points; $\alpha$ and $\beta$ indicate the velocity components; and $c_{\mathbf{q}j}$, $v_{\mathbf{q}j}$, and $\tau_{\mathbf{q}j}$ are heat capacity, group velocity, and relaxation time of the phonon with wave vector $\boldsymbol{q}$ and mode $j$. The phonon relaxation time $\tau_q$ is further given by

$$\begin{aligned}\tau_q^{-1} = \frac{\pi}{N_q \hbar^2} \sum_{\boldsymbol{q}',\boldsymbol{q}''} |V^{(3)}(-\boldsymbol{q};\boldsymbol{q}';\boldsymbol{q}'')|^2 \\ \times [(\bar{n}_{\boldsymbol{q}'} + \bar{n}_{\boldsymbol{q}''} + 1)\delta(\omega_{\boldsymbol{q}} - \omega_{\boldsymbol{q}'} - \omega_{\boldsymbol{q}''}) \\ +2(\bar{n}_{\boldsymbol{q}'} - \bar{n}_{\boldsymbol{q}''})\delta(\omega_{\boldsymbol{q}} + \omega_{\boldsymbol{q}'} - \omega_{\boldsymbol{q}''})],\end{aligned} \tag{2}$$

where $V^{(3)}$ indicates the anharmonicity magnitude of three-phonon scattering; $\bar{n}$ is the Bose-Einstein distribution; and

$\boldsymbol{q}$, $\boldsymbol{q}'$, and $\boldsymbol{q}$ are triplet pairs of three-phonon scattering that satisfy the energy and momentum conservation. The tetrahedron method [36] was used for Brillouin zone integration with $20 \times 20 \times 20$ uniform $q$ mesh. Figure 1(b) shows the calculated thermal conductivity at room temperature using different harmonic and cubic force cutoff distances. For the $4 \times 4 \times 4$ conventional supercell system, the longest interaction can reach the 31st neighbor. Note that as heat conduction in PbTe is isotropic, thermal conductivity is quantified as a scalar value.

With increasing cubic cutoff, the thermal conductivity decreases and converges to almost a constant value of $3.1\,\mathrm{Wm^{-1}K^{-1}}$. When fixing the cubic cutoff at the sixth neighbor and increasing the harmonic force cutoff gradually, the thermal conductivity keeps increasing and finally converges to a constant value at the 28th neighbor. For the commonly used $4 \times 4 \times 4$ primitive supercell system, the reported thermal conductivity is $2.1\,\mathrm{Wm^{-1}K^{-1}}$ [17,22,25], and the corresponding longest interaction length is shorter than the 28th neighbor. This indicates that when calculating the phonon transport in crystals with long range force interaction, the system size and cutoff length should be carefully chosen, otherwise the calculated thermal conductivity will be under- or overestimated. Consequently, the saturated value in the current calculation becomes larger than that in the experiment, which could be attributable to small but non-negligible disorders in the experiment or the selection of the exchange-correlation functions and pseudopotentials in the calculation. The quasiharmonic approximation on calculating the dispersion relations instead of self-consistently including anharmonicity may also be a potential source of uncertainty [37]. Note that although it is possible to post-tune/reason the calculated values to match the experiments, it should not be done at the expense of missing a key physical component; for the purpose of this paper, the somewhat larger value is acceptable.

## III. RESULTS AND DISCUSSION

To study sensitivity of thermal conductivity on the range of resonant bonds, we manipulate the long range harmonic (fourth and eighth neighbor interaction) and anharmonic cubic (the largest first-nearest-neighbor IFCs along [100] direction: $\psi^{xxx}_{PbPbTe}$ and $\psi^{xxx}_{PbTeTe}$, which are only two components out of 633 irreducible cubic IFCs) interaction by scaling the IFCs, as shown in Fig. 2(a). The obtained responses of thermal conductivity to harmonic and cubic IFCs are quite opposite, as shown in Fig. 2(b). The thermal conductivity increases by increasing the range of harmonic interaction, and, in contrast, it decreases with increasing the range of cubic interaction (see Fig. S3 in the Supplemental Material [33] for a similar result when scaling all the components of first and fourth neighbor cubic IFCs). The calculated phonon dispersion relations for typical scaling factors of the fourth and eighth neighbor harmonic interaction are shown in Fig. 3(a). With increasing the scaling factor, the strength of long range interaction increases, and the corresponding TO branches become more dispersive. This trend agrees with the results reported by Lee *et al.* [22], who suggested that the softened TO mode around Γ point reduces thermal conductivity because of enlarging both SPS and anharmonic scattering. However, our result shows that with

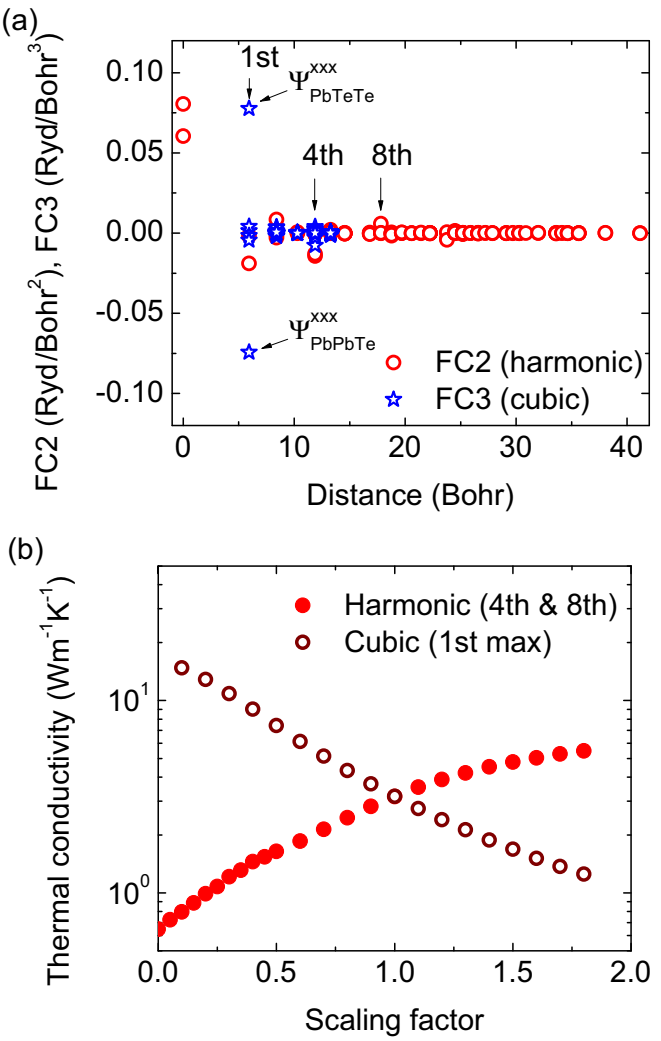


FIG. 2. (a) Harmonic force constants (FC2) and cubic force constants (FC3) versus the neighbor distance. (b) Thermal conductivity versus the scaling factors for FC2 (fourth and eighth neighbor interaction) and FC3 (the largest first-nearest-neighbor interaction along [100] direction: $\psi^{xxx}_{PbPbTe}$ and $\psi^{xxx}_{PbTeTe}$).

softer TO phonons at Γ point, the thermal conductivity of PbTe in fact increases.

To explore and clarify the mechanism behind, the three-phonon SPS [38], which describes the amount of phonon scattering channels, is calculated as

$$P_3(\boldsymbol{q}) = \frac{1}{3m^3}(2P_3^{(+)}(\boldsymbol{q}) + P_3^{(-)}(\boldsymbol{q})), \tag{3}$$

where $m$ is the number of phonon branches, and

$$P_3^{(\pm)}(\boldsymbol{q}) = \frac{1}{N_q}\sum_{\boldsymbol{q}',\boldsymbol{q}''} \delta(\omega_{\boldsymbol{q}} \pm \omega_{\boldsymbol{q}'} - \omega_{\boldsymbol{q}''})\delta_{\boldsymbol{q}\pm\boldsymbol{q}',\boldsymbol{q}''+G}. \tag{4}$$

The total SPS is then given by

$$P_3 = \frac{1}{N_q}\sum_{q} P_3(\boldsymbol{q}). \tag{5}$$

The calculated total SPS and $\Gamma_{TO}$-SPS are shown in Fig. 3(b). $\Gamma_{TO}$-SPS here denotes the partial SPS (subset of $P_3$)

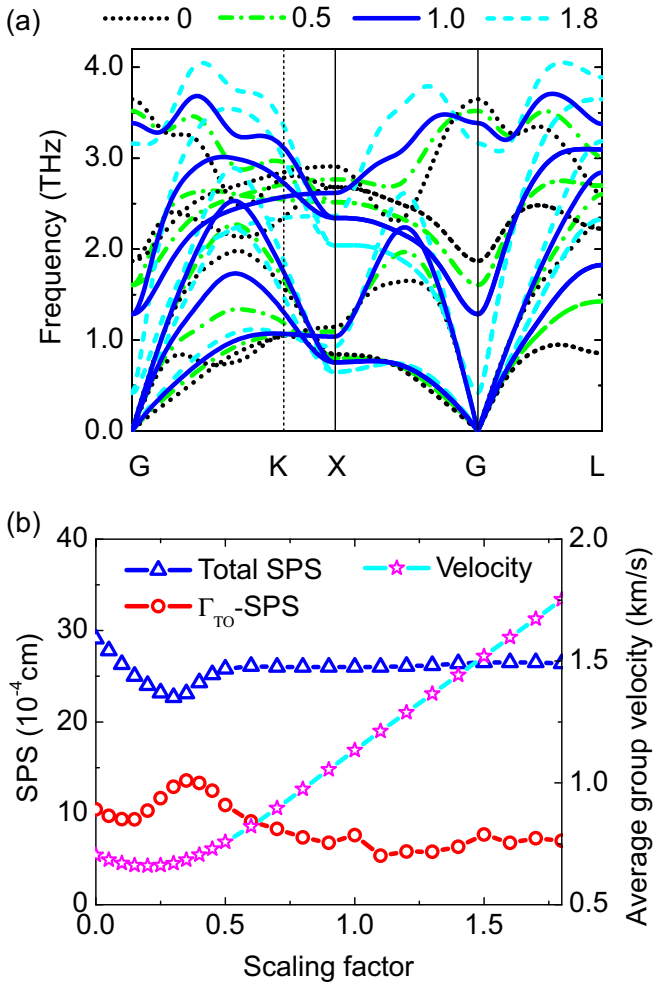


FIG. 3. (a) Phonon dispersion of PbTe with different scaling factors of the fourth and eighth neighbor harmonic force constants. (b) The total and $\Gamma_{TO}$ phonon scattering phase space and average group velocity versus the scaling factors.

of scattering processes involving the TO phonon at the zone center (Γ). The total SPS first decreases to a minimum value at scaling factor of 0.3 and then increases to an almost constant value for scaling factors over 0.5. The $\Gamma_{TO}$-SPS exhibits a similar but opposite trend. Within the range of scaling factors, the thermal conductivity increases monotonically, but the SPS shows a more complicated trend; however, no correlation occurs between SPS and the thermal conductivity.

The plots of mode-dependent thermal conductivity, phonon mean free path (MFP), relaxation time, and group velocity as a function of phonon frequency (see Fig. S4 in the Supplemental Material [33]) are widely used for discussing thermal conductivity from a phonon kinetics viewpoint. Comparing such plots for different scaling factors makes the differences visually unclear because of the fluctuation (i.e., mode dependence), so we instead plot the average group velocity versus the scaling factor in Fig. 3(b). With increasing long range harmonic interaction, the phonon group velocity clearly increases because of more dispersive TO and acoustic phonon branches; therefore, thermal conductivity increases. This indicates that the long

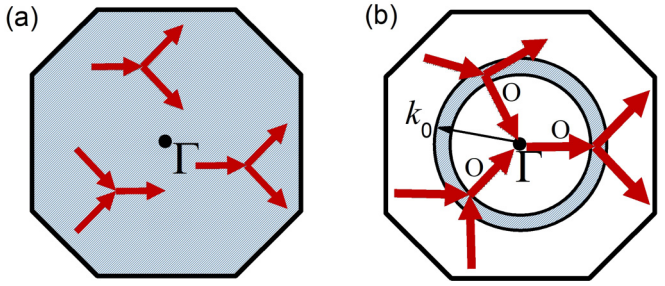


FIG. 4. Sketch of removing specific three-phonon scattering processes: (a) removing scattering of different combinations of three phonons from entire zone; (b) removing three-phonon scattering processes that involve optical phonons with wave vectors of a specific absolute value $k_0 = |\mathbf{k}|$.

range harmonic interaction is not the cause of the low thermal conductivity.

To further explore the mechanism behind the low thermal conductivity of PbTe, we propose an analysis method to quantitatively evaluate the contribution of different three-phonon scattering processes to heat conduction by removing specific scattering processes, as shown in Fig. 4. The thermal conductivity enhancement after removing scattering of different combinations of three phonons is shown in Fig. 5(a). In regard to acoustic (A) and optical (O) phonons, the result indicates

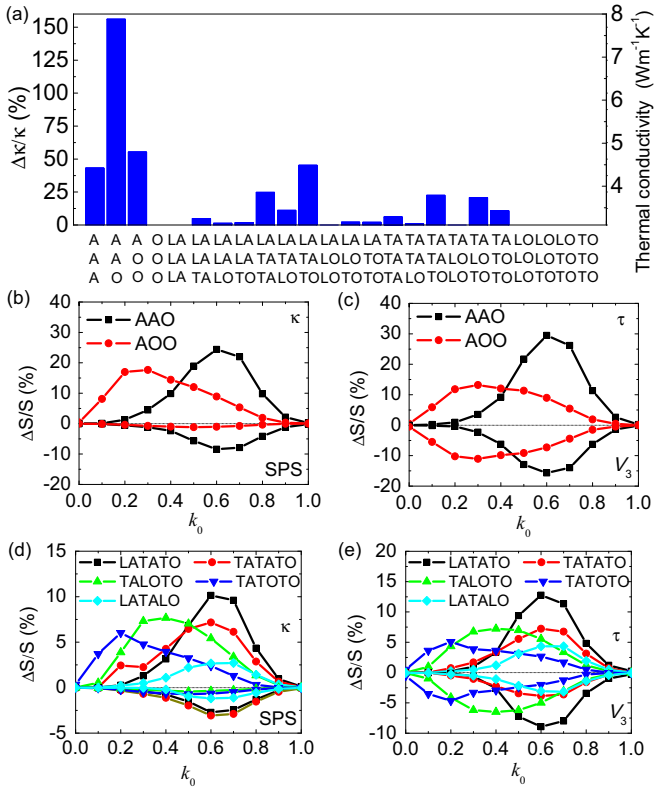


FIG. 5. (a) Thermal conductivity enhancement of PbTe after removing specific three-phonon scattering process. (b)–(e) The variation of thermal conductivity ($\kappa$), scattering phase space (SPS), relaxation time ($\tau$), and anharmonic amplitude ($V_3$) when removing scattering process involving optical phonons with absolute wavevector of $k_0$.

that A-A-O processes (i.e., either creation or annihilation among two A phonons and one O phonon) dominate the heat conduction in PbTe; the next two important processes are A-O-O and A-A-A. In fact, this order of significance is the same as that of partial SPS of the specific three-phonon combination reported previously [22]. However, the current analysis is different from the partial SPS calculation because it also incorporates magnitude of anharmonicity, and we clarify in the following that SPS characteristics are not the reason that these processes impact the thermal conductivity. Figure 5(a) shows a more detailed picture by breaking the processes into those of different polarization, where LA-TA-TO, LA-TA-TA, TA-TA-TO, TA-LO-TO, TA-TO-TO, and LA-TA-LO are found to be the top six processes impacting the thermal conductivity. Four out of six processes involve TO phonons, and thus TO phonons play a leading role; however, as we show in the following, those optical phonons are hardly near-zone-center modes.

The key is to look into the wave vector of phonons that impact scattering properties and thermal conductivity. This was done by removing three-phonon scattering processes that involve optical phonons with wave vectors of a specific absolute value $k_0 = |k|$ [Fig. 4(b)] and by evaluating the resulting variation in the properties. This sensitivity analysis then reveals $k_0$ of phonons that dominantly influence the properties. Figures 5(b) and 5(c) show the variation in thermal conductivity ($\kappa$), SPS, relaxation time ($\tau$), and anharmonic amplitude [estimated by $V_3 \approx 1/(\tau P_3)$] when removing A-A-O and A-O-O scattering processes involving a $k_0$ phonon. In practice, the process is removed if it involves at least one optical phonon with $|k| = k_0$. The result of $\kappa$ in Fig. 5(b) shows that TO phonons near the Γ point play a small role, and it is in fact the phonons with intermediate wave vectors that contribute the most to scattering. For the A-A-O process, the value of dominant $k_0$ normalized by the zone boundary is 0.6, and for A-O-O process it is 0.3. The difference in the peak $k_0$ values between A-A-O and A-O-O processes is understandable because energy conservation limits the A-A-O processes to $A + A \leftrightarrow O$ and the A-O-O processes to $A + O \leftrightarrow O$. Thus, considering the momentum conservation, the optical phonons in the former process end up with larger wave vectors, whereas one of the two optical phonons in the latter can have a relatively smaller wave vector. Nevertheless, none of the peak $k_0$ values are near Γ point, which suggests that the phonon scattering in the entire Brillion zone needs to be characterized on exploring for low thermal conductivity materials.

The profile of $\tau$ in Fig. 5(c) resembles that of $\kappa$, which is reasonable because the harmonic properties and thus group velocities are unchanged during this analysis. Now the issue is whether the variation in relaxation time comes from SPS or anharmonic amplitude ($V_3$), and it is clear by comparing the profiles in terms of the peak position and the amplitude that anharmonic amplitude exhibits much stronger correlation. The stronger correlation is much clearer when further breaking the scattering process by distinguishing phonon polarization, as shown in Figs. 5(d) and 5(e).

## IV. CONCLUSIONS

In summary, we have performed a systematic sensitivity study of PbTe thermal conductivity with respect to the range/magnitude of harmonic and anharmonic IFCs. By increasing the range of harmonic interaction, although TO phonons become softer at Γ point, the thermal conductivity of PbTe increases in relation to what has been previously postulated because of an increase in dispersion and thus group velocity. Sensitivity analysis to the largest nearest neighbor cubic force constants shows that the low thermal conductivity is attributable to their large anharmonicity. Further sensitivity analysis incorporating phonon polarization and wave vector identifies that the low thermal conductivity originates from the magnitude of the anharmonic force constants not through the TO phonons around the zone center but rather dominantly through the larger wave vector TO phonons in the middle of the Brillion zone. This understanding clarifies that the zone-centered TO features, such as band softening and Grüneisen divergence, cannot be used as a direct finger print for low thermal conductivity and that the entire Brillion zone needs to be characterized on exploring low thermal conductivity materials.

## ACKNOWLEDGMENTS

The authors thank Keivan Esfarjani and Terumasa Tadano for useful discussions. The calculations in this paper were performed using supercomputer facilities of the Institute for Solid State Physics, the University of Tokyo. This paper was supported in part by materials research by the Information Integration Initiative ($MI^2I$) project and CREST Grant No. JPMJCR16Q5 from the Japan Science and Technology Agency (JST) and from KAKENHI Grant No. 16H04274 from the Japan Society for the Promotion of Science (JSPS).

[1] J. P. Heremans, V. Jovovic, E. S. Toberer, A. Saramat, K. Kurosaki, A. Charoenphakdee, S. Yamanaka, and G. J. Snyder, Enhancement of thermoelectric efficiency in PbTe by distortion of the electronic density of states, Science **321**, 554 (2008).

[2] O. Delaire, J. Ma, K. Marty, A. F. May, M. A. McGuire, M. H. Du, D. J. Singh, A. Podlesnyak, G. Ehlers, M. D. Lumsden, and B. C. Sales, Giant anharmonic phonon scattering in PbTe, Nat. Mater. **10**, 614 (2011).

[3] G. A. Akhmedova and D. S. Abdinov, Effect of thallium doping on the thermal conductivity of PbTe single crystals, Inorganic Materials **45**, 854 (2009).

[4] J. R. Sootsman, D. Y. Chung, and M. G. Kanatzidis, New and old concepts in thermoelectric materials, Angew Chem. Int. Ed. Engl. **48**, 8616 (2009).

[5] A. A. El-Sharkawy, A. M. Abou El-Azm, M. I. Kenawy, A. S. Hillal, and H. M. Abu-Basha, Thermophysical properties of polycrystalline PbS, PbSe, and PbTe in the temperature range 300–700 K, Int. J. Thermophys. **4**, 261 (1983).

[6] C. B. Vining, W. Laskow, J. O. Hanson, R. R. Van der Beck, and P. D. Gorsuch, Thermoelectric properties of pressure-sintered $Si_{0.8}Ge_{0.2}$ thermoelectric alloys, J. Appl. Phys. **69**, 4333 (1991).

[7] H. R. Meddins and J. E. Parrott, The thermal and thermoelectric properties of sintered germanium-silicon alloys, J. Phys. C: Solid State Phys. **9**, 1263 (1976).

[8] J. Garg and G. Chen, Minimum thermal conductivity in superlattices: A first-principles formalism, Phys. Rev. B **87**, 140302(R) (2013).

[9] S. M. Lee, D. G. Cahill, and R. Venkatasubramanian, Thermal conductivity of Si–Ge superlattices, Appl. Phys. Lett. **70**, 2957 (1997).

[10] Z. Wang, J. E. Alaniz, W. Jang, J. E. Garay, and C. Dames, Thermal conductivity of nanocrystalline silicon: Importance of grain size and frequency-dependent mean free paths, Nano Lett. **11**, 2206 (2011).

[11] S. H. Ju and X. G. Liang, Thermal conductivity of nanocrystalline silicon by direct molecular dynamics simulation, J. Appl. Phys. **112**, 064305 (2012).

[12] J. An, A. Subedi, and D. J. Singh, *Ab initio* phonon dispersions for PbTe, Solid State Commun. **148**, 417 (2008).

[13] O. Kilian, G. Allan, and L. Wirtz, Near Kohn anomalies in the phonon dispersion relations of lead chalcogenides, Phys. Rev. B **80**, 245208 (2009).

[14] Y. Zhang, X. Ke, C. Chen, J. Yang, and P. R. C. Kent, Thermodynamic properties of PbTe, PbSe, and PbS: First-principles study, Phys. Rev. B **80**, 024304 (2009).

[15] W. Cochran, R. A. Cowley, G. Dolling, and M. M. Elcombe, The crystal dynamics of lead telluride, Proc. R. Soc. London A **293**, 433 (1966).

[16] R. M. Murphy, É. D. Murray, S. Fahy, and I. Savić, Broadband phonon scattering in PbTe-based materials driven near ferroelectric phase transition by strain or alloying, Phys. Rev. B **93**, 104304 (2016).

[17] T. Shiga, J. Shiomi, J. Ma, O. Delaire, T. Radzynski, A. Lusakowski, K. Esfarjani, and G. Chen, Microscopic mechanism of low thermal conductivity in lead telluride, Phys. Rev. B **85**, 155203 (2012).

[18] E. S. Bozin, C. D. Malliakas, P. Souvatzis, T. Proffen, N. A. Spaldin, M. G. Kanatzidis, and S. J. Billinge, Entropically stabilized local dipole formation in lead chalcogenides, Science **330**, 1660 (2010).

[19] C. W. Li, O. Hellman, J. Ma, A. F. May, H. B. Cao, X. Chen, A. D. Christianson, G. Ehlers, D. J. Singh, B. C. Sales, and O. Delaire, Phonon Self-Energy and Origin of Anomalous Neutron Scattering Spectra in SnTe and PbTe Thermoelectrics, Phys. Rev. Lett. **112**, 175501 (2014).

[20] Y. Chen, X. Ai, and C. A. Marianetti, First-Principles Approach to Nonlinear Lattice Dynamics: Anomalous Spectra in PbTe, Phys. Rev. Lett. **113**, 105501 (2014).

[21] T. Shiga, T. Murakami, T. Hori, O. Delaire, and J. Shiomi, Origin of anomalous anharmonic lattice dynamics of lead telluride, Appl. Phys. Express **7**, 041801 (2014).

[22] S. Lee, K. Esfarjani, T. Luo, J. Zhou, Z. Tian, and G. Chen, Resonant bonding leads to low lattice thermal conductivity, Nat. Commun. **5**, 3525 (2014).

[23] A. H. Romero, E. K. U. Gross, M. J. Verstraete, and O. Hellman, Thermal conductivity in PbTe from first principles, Phys. Rev. B **91**, 214310 (2015).

[24] S. Kastbjerg, N. Bindzus, M. Søndergaard, S. Johnsen, N. Lock, M. Christensen, M. Takata, M. A. Spackman, and B. Brummerstedt Iversen, Direct evidence of cation disorder in thermoelectric lead chalcogenides PbTe and PbS, Adv. Funct. Mater. **23**, 5477 (2013).

[25] Z. Tian, J. Garg, K. Esfarjani, T. Shiga, J. Shiomi, and G. Chen, Phonon conduction in PbSe, PbTe, and $PbTe_{1-x}Se_x$ from first-principles calculations, Phys. Rev. B **85**, 184303 (2012).

[26] K. Esfarjani, G. Chen, and H. T. Stokes, Heat transport in silicon from first-principles calculations, Phys. Rev. B **84**, 085204 (2011).

[27] K. Esfarjani and H. T. Stokes, Method to extract anharmonic force constants from first principles calculations, Phys. Rev. B **77**, 144112 (2008).

[28] P. Giannozzi, S. Baroni, N. Bonini, M. Calandra, R. Car, C. Cavazzoni, D. Ceresoli, G. L. Chiarotti, M. Cococcioni, I. Dabo, A. Dal Corso, S. de Gironcoli, S. Fabris, G. Fratesi, R. Gebauer, U. Gerstmann, C. Gougoussis, A. Kokalj, M. Lazzeri, L. Martin-Samos *et al.*, QUANTUM ESPRESSO: a modular and open-source software project for quantum simulations of materials, J. Phys.: Condens. Matter **21**, 395502 (2009).

[29] T. Tadano, Y. Gohda, and S. Tsuneyuki, Anharmonic force constants extracted from first-principles molecular dynamics: applications to heat transfer simulations, J. Phys.: Condens. Matter **26**, 225402 (2014).

[30] X. Gonze, Perturbation expansion of variational principles at arbitrary order, Phys. Rev. A **52**, 1086 (1995).

[31] X. Gonze, Adiabatic density-functional perturbation theory, Phys. Rev. A **52**, 1096 (1995).

[32] S. Baroni, P. Giannozzi, and A. Testa, Green's-Function Approach to Linear Response in Solids, Phys. Rev. Lett. **58**, 1861 (1987).

[33] See Supplemental Material at http://link.aps.org/supplemental/10.1103/PhysRevB.97.184305 for (i) phonon dispersion using different supercell size; (ii) comparison of TO frequency at zone center using different supercell size with DFPT calculation result; (iii) thermal conductivity versus the scaling factors for different components of cubic IFCs; and (iv) mode-dependent thermal conductivity, mean free path, relaxation time, and group velocity as a function of phonon frequency for typical scaling factors for harmonic fourth and eighth IFCs.

[34] G. P. Srivastava, Anharmonic relaxation of phonons, Pramana **3**, 209 (1974).

[35] D. A. Broido, M. Malorny, G. Birner, N. Mingo, and D. A. Stewart, Intrinsic lattice thermal conductivity of semiconductors from first principles, Appl. Phys. Lett. **91**, 231922 (2007).

[36] P. E. Blöchl, O. Jepsen, and O. K. Andersen, Improved tetrahedron method for Brillouin-zone integrations, Phys. Rev. B **49**, 16223 (1994).

[37] G. A. S. Ribeiro, L. Paulatto, R. Bianco, I. Errea, F. Mauri, and M. Calandra, Strong anharmonicity in the phonon spectra of PbTe and SnTe from first principles, Phys. Rev. B **97**, 014306 (2018).

[38] L. Lindsay and D. A. Broido, Three-phonon phase space and lattice thermal conductivity in semiconductors, J. Phys.: Condens. Matter **20**, 165209 (2008).